HHS Public Access

Author manuscript

Nature. Author manuscript; available in PMC 2012 April 04.

Published in final edited form as:

Nature. ; 474(7353): 645–648. doi:10.1038/nature10094.

Latent TGFβ binding protein 3 identifies a second heart field in zebrafish

Yong Zhou[1,2], **Timothy J. Cashman**[1,2], **Kathleen R. Nevis**[1,2], **Pablo Obregon**[1,2], **Sara A. Carney**[3], **Yan Liu**[2,4], **Aihua Gu**[1,2,5], **Christian Mosimann**[2,6], **Samuel Sondalle**[1,2,7], **Richard E. Peterson**[3], **Warren Heideman**[3], **Caroline E. Burns**[1,2,7,*], and **C. Geoffrey Burns**[1,2,*]

[1]Cardiovascular Research Center, Massachusetts General Hospital, Charlestown, MA 02129

[2]Harvard Medical School, Boston, MA 02115

[3]Pharmaceutical Sciences Division, School of Pharmacy, University of Wisconsin, Madison, WI, 53705

[4]Nephrology Division, Massachusetts General Hospital, Charlestown, MA 02129

[5]School of Public Health, Nanjing Medical University, Nanjing, 210029, China

[6]Stem Cell Program and Division of Hematology/Oncology, Children's Hospital Boston, MA 02115

[7]Harvard Stem Cell Institute, Cambridge, MA 02138

Abstract

The four-chambered mammalian heart develops from two fields of cardiac progenitor cells (CPCs) distinguished by their spatiotemporal patterns of differentiation and contributions to the definitive heart [1–3]. The first heart field differentiates earlier in lateral plate mesoderm, generates the linear heart tube and ultimately gives rise to the left ventricle. The second heart field (SHF) differentiates later in pharyngeal mesoderm, elongates the heart tube, and gives rise to the outflow tract (OFT) and much of the right ventricle. Because hearts in lower vertebrates contain a rudimentary OFT but not a right ventricle [4], the existence and function of SHF-like cells in these species has remained a topic of speculation [4–10]. Here we provide direct evidence from Cre/Lox-mediated lineage tracing and loss of function studies in zebrafish, a lower vertebrate with a single ventricle, that *latent-TGFβ binding protein 3 (ltbp3)* transcripts mark a field of CPCs with defining characteristics of the anterior SHF in mammals. Specifically, *ltbp3*$^{+}$ cells differentiate in

*Correspondence and requests for materials should be addressed to C.E.B. (cburns6@partners.org) and/or C.G.B. (cburns@crvc.mgh.harvard.edu).

Supplementary Information is linked to the online version of the paper at www.nature.com/nature.

Author Contributions Y.Z. performed the majority of the experiments and analyzed data; T.C., K.N., P.O, Y.L., A.G, and S.S. performed experiments and analyzed data; C.M. provided the ubiquitin promoter prior to publication; S.C., R.P., W.H. and C.G.B. discovered that *ltbp3* transcripts are upregulated in a cardiac fraction on day 3 post fertilization; C.G.B performed experiments including BAC recombineering; C.E.B. and C.G.B. co-directed the study, analyzed data, and wrote the paper with input from all authors.

Author Information The zebrafish *ltbp3* cDNA sequence was deposited into GenBank under accession number JF731042.

The authors declare no competing financial interests.

pharyngeal mesoderm after formation of the heart tube, elongate the heart tube at the outflow pole, and give rise to three cardiovascular lineages in the OFT and myocardium in the distal ventricle. In addition to expressing Ltbp3, a protein that regulates the bioavailability of TGFβ ligands [11], zebrafish SHF cells co-express *nkx2.5*, an evolutionarily conserved marker of CPCs in both fields [4]. Embryos devoid of *ltbp3* lack the same cardiac structures derived from *ltbp3*$^{+}$ cells due to compromised progenitor proliferation. Additionally, small-molecule inhibition of TGFβ signaling phenocopies the *ltbp3*-morphant phenotype whereas expression of a constitutively active TGFβ type I receptor rescues it. Taken together, our findings uncover a requirement for *ltbp3*-TGFβ signaling during zebrafish SHF development, a process that serves to enlarge the single ventricular chamber in this species.

Using *in situ* hybridization, we discovered that zebrafish *ltbp3* transcripts are expressed in cells at the outflow pole of the linear heart tube (Fig. 1a, b and Supplementary Fig. 1 and 2). Double marker analyses confirmed that a majority of *ltbp3*$^{+}$ cells are non-overlapping with differentiated myocardium (Fig. 1c–e and Supplementary Fig. 2). Additionally, *ltbp3*$^{+}$ cells are neither endothelial nor derived from the neural crest because *ltbp3* expression remains robust in embryos lacking both cell types (Supplementary Fig. 3). Because the anatomical relationship of *ltbp3*$^{+}$ cells to the heart tube is reminiscent of the anterior segment of the SHF in mice [3, 12], *ltbp3*$^{+}$ cells were evaluated for co-expression of *nkx2.5*, an evolutionarily conserved marker of CPCs in both heart fields [4]. As reported previously, cells in the linear heart tube were positive for *nkx2.5* [13]. Surprisingly, *nkx2.5* expression also overlapped with *ltbp3* transcripts demonstrating that an extra-cardiac population of *ltbp3*$^{+}$, *nkx2.5*$^{+}$ cells resides at the outflow pole of the zebrafish heart tube (Fig. 1f–h). This population was also readily identified in double transgenic *Tg(nkx2.5*^{BAC}*::ZsYellow); Tg(cmlc2::CSY)* embryos expressing ZsYellow and AmCyan proteins from *nkx2.5* and myocardial (*cmlc2*) promoters respectively (Fig. 1o–q). Lastly, these cells co-express zebrafish *tgfβ3* transcripts (Supplementary Fig. 4) consistent with the demonstrated function of LTBP proteins as regulators of TGFβ signaling [11].

To determine if *Ltbp3* is required for zebrafish cardiogenesis, we evaluated embryos injected with anti-sense *ltbp3* morpholinos (*MO*^{ltbp3}; Supplementary Fig. 5) for chamber-specific defects in cardiomyocyte and endocardial cell number. Knocking down *ltbp3* halved the number of ventricular cardiomyocytes and endocardial cells, while atrial cell numbers were unaffected (Fig. 2a–f). The ventricular deficit was evident earlier in development, soon after formation of the heart tube, as shortening of the ventricular segment accompanied by a defect in cardiac looping (Fig. 2g–i). *MO*^{ltbp3} animals also lacked Eln2^{+} OFT smooth muscle precursor cells (Fig. 2j–m) [7, 14] homologous to SHF-derived smooth muscle surrounding the base of the aorticopulmonary trunk in higher vertebrates [10]. Lastly, *ltbp3* morphants failed to form the ventral aorta (data not shown) and a majority of pharyngeal arch arteries (Supplementary Fig. 6). Taken together, these data demonstrate that knocking down *ltbp3* causes multi-lineage cardiovascular defects in the pharyngeal arches, OFT, and ventricle.

In mammals, the anterior segment of the SHF gives rise to the embryonic OFT and the right ventricular half of the common embryonic ventricle prior to septation [1–3]. Despite the fact

that zebrafish embryos never septate their single ventricles, the *MO*^{ltbp3} phenotype is remarkably similar to mouse anterior SHF mutants that die prior to septation with severe reductions in the primitive right ventricle and OFT [15–17]. Therefore, we tested the hypothesis that *ltbp3*$^{+}$ cells represent a SHF-like population that gives rise to some or all of the structures missing in *MO*^{ltbp3} embryos. To that end, we used Cre/Lox-mediate lineage tracing to irreversibly mark *ltbp3*$^{+}$ cells and their descendents that assume myocardial, endocardial/endothelial, and smooth muscle cell fates. First, we derived a transgenic driver strain, *Tg(ltbp3::TagRFP2Acre)*, that co-expresses a red fluorescent protein (*TagRFP*) and Cre recombinase in *ltbp3*$^{+}$ cells (Fig. 3a and Supplementary Fig. 7). Secondly, we generated three lineage-restricted reporter strains that carry a unique Cre-responsive "color switching" cassette (AmCyan-Switch-ZsYellow; CSY) under transcriptional control of myocardial (*cmlc2*), endothelial (*kdrl*), and smooth muscle precursor cell (*eln2*) [7, 14] promoters (Fig. 3b and Supplementary Fig. 8). We also generated a ubiquitous reporter strain using the zebrafish ubiquitin promoter [18] (Fig. 3b and Supplementary Fig.8). For each reporter, we confirmed Cre-dependent AmCyan to ZsYellow "color switching" caused by excision of the floxed AmCyan-STOP sequence from the reporter cassette (Supplementary Fig. 8).

Double transgenic progeny from the driver and myocardial reporter strains expressed ZsYellow protein in approximately the distal half of the ventricle (Fig. 3c) demonstrating that myocardium in this segment of the ventricle descends from *ltbp3*$^{+}$ progenitors. Myocardial cells in the proximal OFT also arise from *ltbp3*$^{+}$ cells (Supplementary Fig. 9). Furthermore, *MO*^{ltbp3} ventricles lacked *ltbp3*$^{+}$ cell derived cardiomyocytes confirming that the distal ventricle is specifically affected in morphant embryos (Fig. 3d). In higher vertebrates, SHF cells labeled with a tracking dye after heart tube formation migrate into the OFT tract and ventricle [12, 19, 20]. Similarly, we injected CellTrackerRed into the non-myocardial (AmCyan^{-}), *nkx2.5*$^{+}$ (ZsYellow^{+}) region of double transgenic *Tg(nkx2.5*^{BAC}*::ZsYellow); Tg(cmlc2::CSY)* embryos at the heart tube stage and observed subsequent dye migration into the distal ventricle and OFT (Fig. 3 e–h). Taken together, these data demonstrate that *ltbp3*$^{+}$ cells give rise to distal ventricular myocardium through late differentiation and accretion to the heart tube.

By crossing our driver line with the endothelial and smooth muscle reporter strains, we learned that *ltbp3*-expressing cells also give rise to endothelial and smooth muscle cells in the OFT (Fig. 3i, j). In smooth muscle reporter embryos, ZsYellow fluorescence was predominantly observed at the base of the OFT (Fig. 3j), suggesting that *ltbp3*$^{+}$ cells make a regionalized contribution to OFT smooth muscle. We did not observe color switching in ventricular endocardium or pharyngeal arch artery endothelium suggesting that these cellular compartments do not derive from *ltbp3*$^{+}$ cells (data not shown). Finally, lineage tracing *ltbp3*$^{+}$ cells with the ubiquitous reporter corroborated the conclusions drawn from lineage-restricted reporters (Fig. 3k–n). Taken together, these data demonstrate that *ltbp3*$^{+}$ cells, in addition to giving rise to ventricular myocardium, also give rise to three cardiovascular lineages in the OFT.

To elucidate the cellular mechanism(s) underlying the *MO*^{ltbp3} phenotype, we evaluated *MO*^{ltbp3} embryos, soon after formation of the heart tube, for cellular defects in the extra-cardiac population of *ltbp3*$^{+}$, *nkx2.5*$^{+}$ cells at its outflow pole. Although *TagRFP*-expressing

ltbp3^{+} cells are too faint to visualize in *Tg(ltbp3::TagRFP2Acre)* embryos at this developmental stage, non-myocardial ZsYellow-expressing *nkx2.5*$^{+}$ cells are readily detected in *Tg(nkx2.5::ZsYellow); Tg(cmlc2::CSY)* embryos (Fig. 1o–q). Shortly after heart tube formation, both control and *MO*^{ltbp3} embryos harbored extra-cardiac *nkx2.5*$^{+}$ cells demonstrating that progenitor specification is not compromised by loss of *ltbp3* function (Fig. 3o, p). However, eleven hours later, this population was absent specifically in *MO*^{ltbp3} animals (Fig. 3q, r). The absence of TUNEL staining suggested strongly that progenitor survival is not compromised (data not shown). By contrast, BrdU staining revealed that progenitor proliferation is significantly reduced in *MO*^{ltbp3} embryos (Fig. 3s–u). Taken together, these data support a model in which *ltbp3* functions in an autocrine fashion to stimulate proliferation or self-renewal of *ltbp3*$^{+}$, *nkx2.5*$^{+}$, progenitors to sustain adequate CPC numbers during their differentiation and migration from the SHF. Based on this model, we speculate that knocking down *ltbp3* causes a premature depletion of CPCs from the SHF.

LTBP proteins are secreted with TGFβ ligands in a large latent complex (LLC) that becomes anchored to the extracellular matrix prior to ligand activation [11]. Because LTBP proteins are also required for secretion of TGFβ ligands, we used three approaches to test the hypothesis that defective TGFβ signaling underlies the cardiovascular phenotypes seen in *MO*^{ltbp3} embryos. First, we evaluated the linear heart tube and surrounding regions for phosphorylated pSmad2 epitopes, a hallmark of active TGFβ signaling [21]. TGFβ signaling was observed in the heart tube proper and in extra-cardiac cells approximating the location of *ltbp3*$^{+}$, *nkx2.5*$^{+}$ progenitors (Fig. 4a). Loss of *ltbp3* function eliminated pSmad2 epitopes specifically in the extra-cardiac population leaving signaling in the heart tube unaffected. These data demonstrate that morphant embryos exhibit a highly localized defect in TGFβ signaling specifically in the SHF (Fig. 4B). Next, we evaluated whether small molecule inhibition of TGFβ signaling would phenocopy *MO*^{ltbp3} animals. To that end, we used a selective inhibitor (LY-364947; [22]) of the TGFβ type I receptor ALK5 that effectively abrogated TGFβ signaling in zebrafish embryos (Fig 4c). LY-364947-treated animals phenocopied *ltbp3* morphants as evidenced by reductions in *ltbp3*$^{+}$ cell derived myocardium and OFT smooth muscle (Fig. 4d–g). Using LY-364947, we also determined the developmental time window, 26–36 hours post-fertilization during which TGFβ signaling is required for the formation of the distal ventricle (Supplementary Fig. 10), the same time window during which *nkx2.5*$^{+}$ progenitors disappear in *MO*^{ltbp3} embryos (Fig. 3o–r). Lastly, we attempted to rescue *MO*^{ltbp3} embryos by inducing ubiquitous expression of a constitutively active TGFβ-type I receptor (caALK5), the same receptor targeted by LY-364947, predicted to be downstream of *ltbp3* and TGFβ ligands (Supplementary Fig. 9). In a majority of embryos, heat-shock inducible expression of caALK5 partially or fully rescued the loss of distal myocardium seen in *MO*^{ltbp3} embryos (Fig. 4h–j). Taken together, these results suggest that attenuation of TGFβ signaling underlies the cardiovascular phenotypes present in *MO*^{ltbp3} embryos.

Because *ltbp3*$^{+}$ cells differentiate after formation of the heart tube in pharyngeal mesoderm, elongate the tube at the outflow pole, and give rise to three cardiovascular lineages in the OFT and myocardium in the distal ventricle, they exhibit defining characteristics of the

mouse anterior SHF. As such, *ltbp3*$^{+}$ cells would also be predicted to encompass the zebrafish equivalents of the avian secondary and anterior heart fields [1, 19, 23].

Our findings are consistent with a recent study demonstrating that pre-existing ventricular cardiomyocytes do not give rise to new cardiomyocytes during elongation of the zebrafish heart tube [9]. The same authors report that the zebrafish homolog of *Islet1*, a well-known marker of mammalian SHF cells, is dispensable for formation of the distal ventricle, herein reported to derive from the zebrafish SHF. Thus, it appears that the critical role of *Islet1*, during anterior SHF development, has become minimized or replaced by another factor specifically in the fish lineage. Alternatively, *Islet1* function during mammalian anterior SHF development might have co-evolved with the four-chambered heart [24].

Although zebrafish do not have a right ventricle, *ltbp3*$^{+}$ cells accrete the distal ventricular segment to the zebrafish heart tube much like SHF cells accrete the primitive right ventricle to the mouse heart tube prior to septation. In mouse, the SHF-derived segment becomes a distinct chamber after septation. In zebrafish, the SHF-derived segment instead augments the singular ventricular chamber, a trait that may have conferred an evolutionary advantage to a common ancestor of both zebrafish and mammals.

Methods Summary

Single and double, fluorescent and non-fluorescent, *in situ hybridization* and immunohistochemical stainings were performed using standard protocols. To analyze the *ltbp3* loss of function phenotype, we injected anti-sense *ltbp3* morpholinos into one-cell stage WT and transgenic embryos. For genetic lineage tracing, a transgenic driver strain expressing Cre recombinase in *ltbp3*$^{+}$ cells and four Cre-responsive “color switching” reporter strains were generated using standard methods. The driver strain was crossed individually to each of the reporter strains and their double transgenic progenies were analyzed for ZsYellow protein fluorescence using confocal microscopy. To follow the migration of zebrafish SHF cells, a tracking dye was injected into the ZsYellow^{+}, AmCyan^{-} region of *Tg(nkx2.5::ZsYello); Tg(cmlc2::CSY)* embryos at 24hpf, the embryos were imaged immediately, and then again at 48 and/or 72hpf. A transgenic strain carrying a cDNA encoding a constitutively active human TGFβ type I receptor (caALK5) under control of the zebrafish heat shock promoter was generated and used to rescue the myocardial defect in *ltbp3* morphant embryos.

Full Methods and any associated references are available in the online version of the paper at www.natre.com/nature

Supplementary Material

Refer to Web version on PubMed Central for supplementary material.

Acknowledgements

We thank M. Whitman for advice on pSmad2 staining, D. Hami and M. Kirby for providing Eln2 anti-sera and their immunohistochemistry protocol, R. Cornell for providing *tfAP2a* and *tfAP2c* morpholinos, M. Whitman, A. Srinivasan, D. Langenau, E. Provost, S. Leach, R. Anderson, D. Stainier, I.Woods, and A. Schier for providing

plasmids. J.W. Xiong for providing *clo*^{m39} fish, B. Barut and L. Zon for providing BACs, and the MGH Nephrology Division for access to their confocal microscopy facilities. S.C., R.E.P., and W.H. were supported by NIH grant R01 ES012716 from the National Institute of Environmental Health Sciences. C.M. received support through an EMBO long-term fellowship and a HFSP long-term fellowship. This work was funded by the Cardiovascular Research Center at Massachusetts General Hospital, a Claflin Distinguished Scholar Award and Harvard Stem Cell Institute Seed Grant to C.E. Burns, and by awards from the National Heart Lung and Blood Institute (5R01HL096816), American Heart Association (Grant in Aid # 10GRNT4270021), and Harvard Stem Cell Institute (Seed Grant) to C.G. Burns.

References

1. Dyer LA, Kirby ML. The role of secondary heart field in cardiac development. Dev Biol. 2009; 336(2):137–144. [PubMed: 19835857]
2. Rochais F, Mesbah K, Kelly RG. Signaling pathways controlling second heart field development. Circ Res. 2009; 104(8):933–942. [PubMed: 19390062]
3. Vincent SD, Buckingham ME. How to make a heart: the origin and regulation of cardiac progenitor cells. Curr Top Dev Biol. 2010; 90:1–41. [PubMed: 20691846]
4. Olson EN. Gene regulatory networks in the evolution and development of the heart. Science. 2006; 313(5795):1922–1927. [PubMed: 17008524]
5. Cai CL, et al. Isl1 identifies a cardiac progenitor population that proliferates prior to differentiation and contributes a majority of cells to the heart. Dev Cell. 2003; 5(6):877–889. [PubMed: 14667410]
6. Meilhac SM, et al. The clonal origin of myocardial cells in different regions of the embryonic mouse heart. Dev Cell. 2004; 6(5):685–698. [PubMed: 15130493]
7. Grimes AC, et al. Solving an enigma: arterial pole development in the zebrafish heart. Dev Biol. 2006; 290(2):265–276. [PubMed: 16405941]
8. Brade T, et al. The amphibian second heart field: Xenopus islet-1 is required for cardiovascular development. Dev Biol. 2007; 311(2):297–310. [PubMed: 17900553]
9. de Pater E, et al. Distinct phases of cardiomyocyte differentiation regulate growth of the zebrafish heart. Development. 2009; 136(10):1633–1641. [PubMed: 19395641]
10. Grimes AC, et al. Phylogeny informs ontogeny: a proposed common theme in the arterial pole of the vertebrate heart. Evol Dev. 2010; 12(6):552–567. [PubMed: 21040422]
11. Rifkin DB. Latent transforming growth factor-beta (TGF-beta) binding proteins: orchestrators of TGF-beta availability. J Biol Chem. 2005; 280(9):7409–7412. [PubMed: 15611103]
12. Kelly RG, Brown NA, Buckingham ME. The arterial pole of the mouse heart forms from Fgf10-expressing cells in pharyngeal mesoderm. Dev Cell. 2001; 1(3):435–440. [PubMed: 11702954]
13. Chen JN, et al. Left-right pattern of cardiac BMP4 may drive asymmetry of the heart in zebrafish. Development. 1997; 124(21):4373–4382. [PubMed: 9334285]
14. Miao M, et al. Differential expression of two tropoelastin genes in zebrafish. Matrix Biol. 2007; 26(2):115–124. [PubMed: 17112714]
15. Ilagan R, et al. Fgf8 is required for anterior heart field development. Development. 2006; 133(12): 2435–2445. [PubMed: 16720880]
16. Prall OW, et al. An Nkx2-5/Bmp2/Smad1 negative feedback loop controls heart progenitor specification and proliferation. Cell. 2007; 128(5):947–959. [PubMed: 17350578]
17. von Both I, et al. Foxh1 is essential for development of the anterior heart field. Dev Cell. 2004; 7(3):331–345. [PubMed: 15363409]
18. Mosimann C, et al. Ubiquitous transgene expression and Cre-based recombination driven by the ubiquitin promoter in zebrafish. Development. 2010; 138(1):169–177. [PubMed: 21138979]
19. Waldo KL, et al. Conotruncal myocardium arises from a secondary heart field. Development. 2001; 128(16):3179–3188. [PubMed: 11688566]
20. Zaffran S, et al. Right ventricular myocardium derives from the anterior heart field. Circ Res. 2004; 95(3):261–268. [PubMed: 15217909]
21. Todorovic V, et al. Long form of latent TGF-beta binding protein 1 (Ltbp1L) is essential for cardiac outflow tract septation and remodeling. Development. 2007; 134(20):3723–3732. [PubMed: 17804598]

22. Li HY, et al. Dihydropyrrolopyrazole transforming growth factor-beta type I receptor kinase domain inhibitors: a novel benzimidazole series with selectivity versus transforming growth factor-beta type II receptor kinase and mixed lineage kinase-7. J Med Chem. 2006; 49(6):2138–2142. [PubMed: 16539403]

23. Mjaatvedt CH, et al. The outflow tract of the heart is recruited from a novel heart-forming field. Dev Biol. 2001; 238(1):97–109. [PubMed: 11783996]

24. Kang J, et al. Isl1 is a direct transcriptional target of Forkhead transcription factors in second-heart-field-derived mesoderm. Dev Biol. 2009; 334(2):513–522. [PubMed: 19580802]

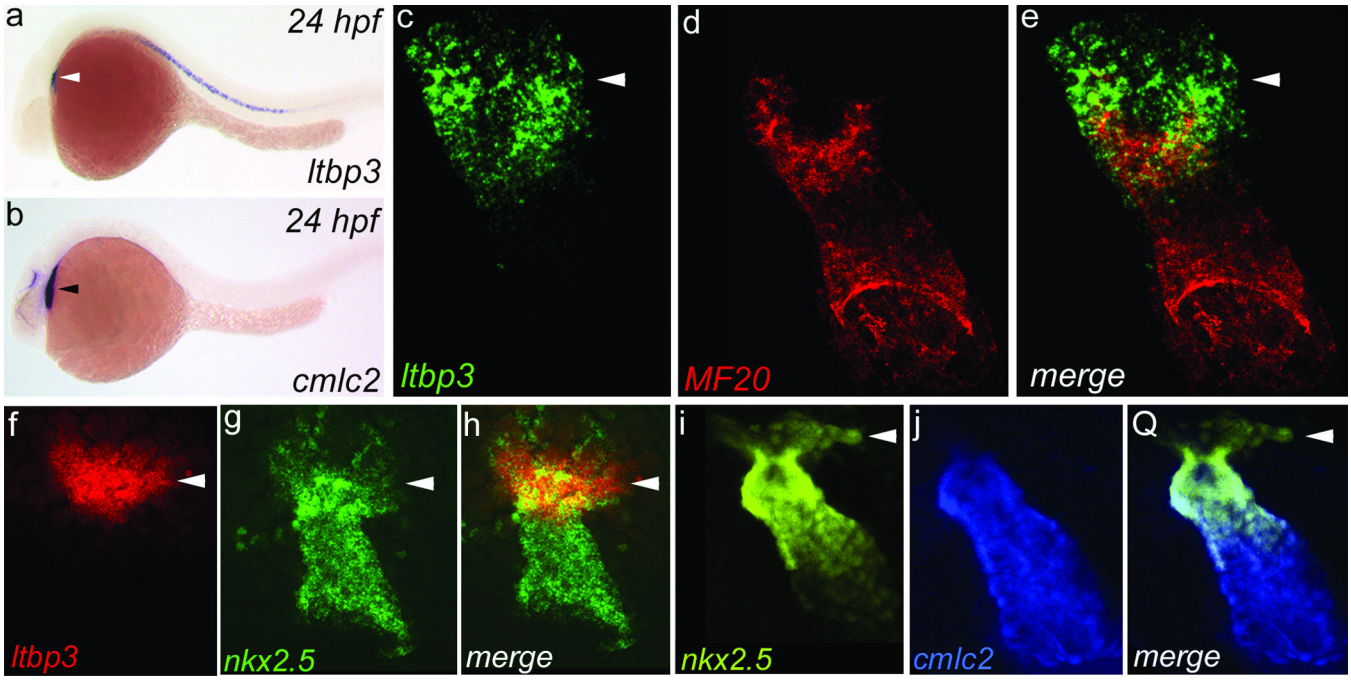

Figure 1. *ltbp3* and *nkx2.5* transcripts mark extra-cardiac cells contiguous to the outflow pole of the zebrafish heart tube

a,b, *ltbp3*$^{+}$ cells (white arrowhead) visualized by *in situ hybridization* at 24 hours post-fertilization (hpf) reside dorsal to the *cmlc2*$^{+}$ heart tube (black arrowhead; n=15+ embryos/group). **c–e,** Heart tube region in 24 hpf embryo co-stained with *ltbp3*$^{+}$ riboprobe (green; arrowhead) and a muscle-specific antibody (MF20; red; n=3/3) that recognizes cardiomyocytes. **f–h,** Heart tube region in 24 hpf embryo co-stained with *ltbp3* and *nkx2.5* riboprobes highlighting *ltbp3*$^{+}$, *nkx2.5*$^{+}$ cells (arrowheads) at the outflow pole of the heart tube (n=9/9). **i–k,** Heart tube region in 26 hpf *Tg(nkx2.5::ZsYellow); Tg(cmlc2::CSY)* embryo highlighting non-myocardial *nkx2.5*$^{+}$ cells (arrowheads).

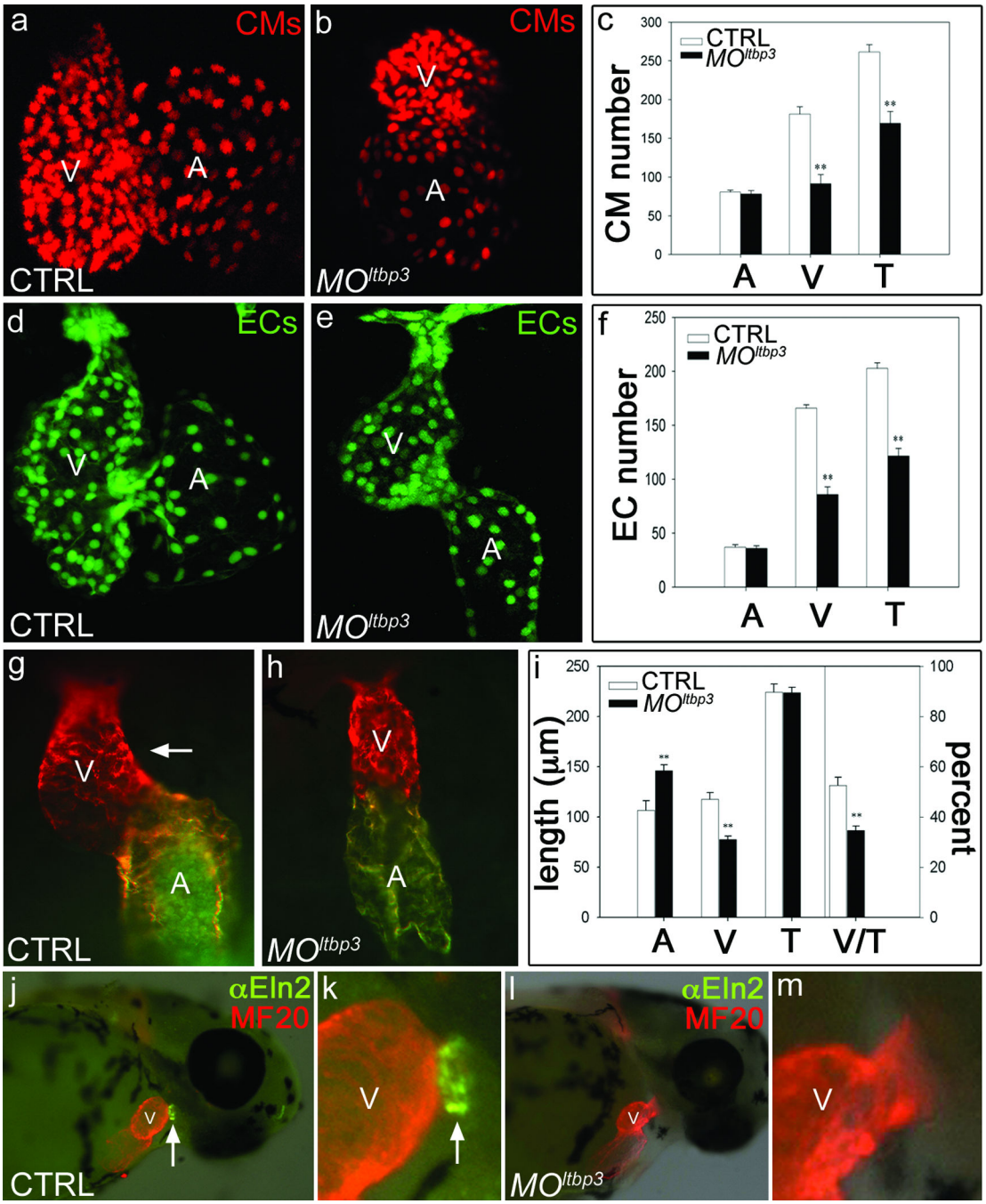

Figure 2. Knocking down *ltbp3* causes multi-lineage cardiovascular defects in the ventricle and OFT

a–f, Cardiomyocyte (CM) and endocardial (EC) cell numbers in control and *MO*^{ltbp3} atria (A) and ventricles (V) at 72 hpf in *cmlc2::dsRed2-nuc* and *fli1::nEGFP* embryos (n=6/group, T=total) **g–i,** Atrial (A) and ventricular (V) segment lengths in control and *MO*^{ltbp3} embryos at 36hpf (n=9/group; white arrow highlights rightward looping of the ventricle in control embryos). Error bars in all graphs represent 1 s.d., ** p<0.01. **j–m,** 60 hpf control

and *MO*^{ltbp3} embryos stained with α-Eln2 antibodies (n=24/24 for WT; 28/31 for *MO*^{ltbp3}) that recognize OFT smooth muscle cell precursor cells (white arrow).

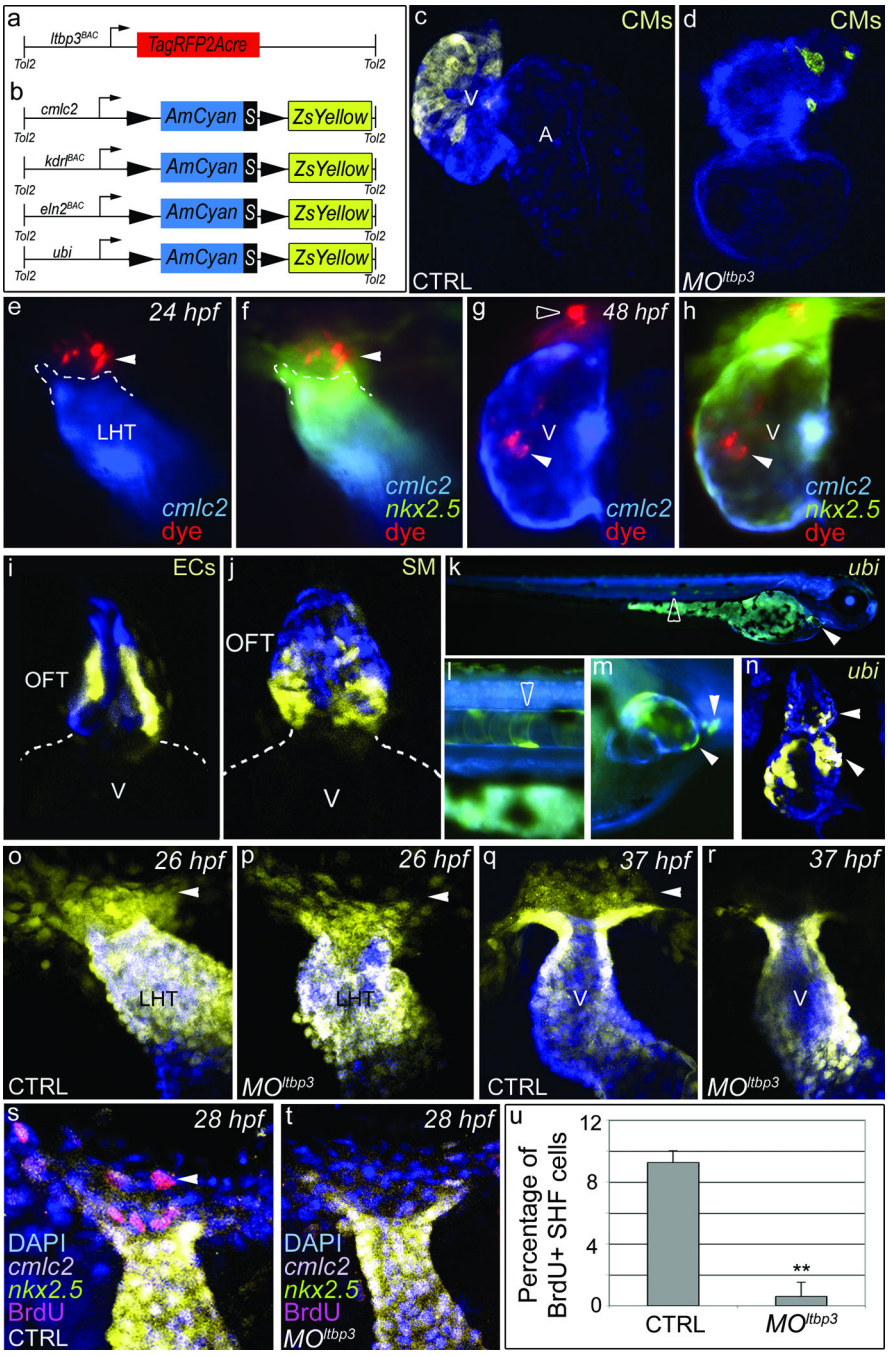

Figure 3. *ltbp3*$^{+}$ cells give rise to three cardiovascular lineages in the zebrafish ventricle and OFT

a,b, Schematic of driver (A) and reporter (B) transgenes. **c,d,** *Tg(ltbp3::TagRFP2Acre); Tg(cmlc2::CSY)* control and *MO*^{ltbp3} hearts at 72 hpf (n=>20/group; >90% exhibited ZsYellow distribution shown). **e–h,** 24 hpf *Tg(nkx2.5*^{BAC}*::ZsYellow); Tg(cmlc2::CSY)* embryo injected with tracking dye (arrowheads) in non-myocardial *nkx2.5*$^{+}$ region imaged again at 48 hpf. The dye tracked to the distal ventricle (7/16 embryos accurately injected), the myocardial segment of the OFT (5/16; not shown), and both structures (6/16) respectively. Black arrowhead highlights dye that failed to migrate. **i,** OFT region in

Tg(ltbp3::TagRFP2Acre); Tg(kdrl::CSY) embryo at 6 days post fertilization (dpf) [n=16, >50% exhibited ZsYellow fluorescence in OFT endothelial cells (ECs)]. **j,** OFT region in *Tg(ltbp3::TagRFP2Acre); Tg(eln2::CSY)* embryo at 7 dpf [n=12, >80% of exhibited ZsYellow fluorescence in OFT smooth muscle (SM) precursors]. **k–n,** *Tg(ltbp3::TagRFP2Acre); Tg(ubi::CSY)* embryo at 4 dfp (**k–m**) and confocal section of the heart on 6 dpf (**n**) [n=12, >90% of embryos exhibited ZsYellow protein in the distal ventricle (white arrowhead) and OFT (white arrowhead)]. Open arrowheads highlight color switching in the *ltbp3+* notochord. **o–r,** Heart tube regions in control and MO^{ltbp3} *Tg(nkx2.5::ZsYellow, cmlc2::CSY)* embryos at 26 and 37 hpf. Arrows indicate non-myocardial $nkx2.5^{+}$ cells present in all experimental groups except MO^{ltbp3} animals at 37hpf (n=18/18 and 12/12 for control and morphants respectively). **s-u,** 28 hpf control and MO^{ltbp3} *Tg(nkx2.5::ZsYellow); Tg(cmlc2::CSY)* embryos, processed for DAPI and BrDU staining. The percentages of BrdU+ cells in the ZsYellow+, AmCyan− region are shown in **u** (n=6 embryos/group, one s.d. is shown, ** $p<0.01$). V=ventricle, A=atrium, LHT=linear heart tube.

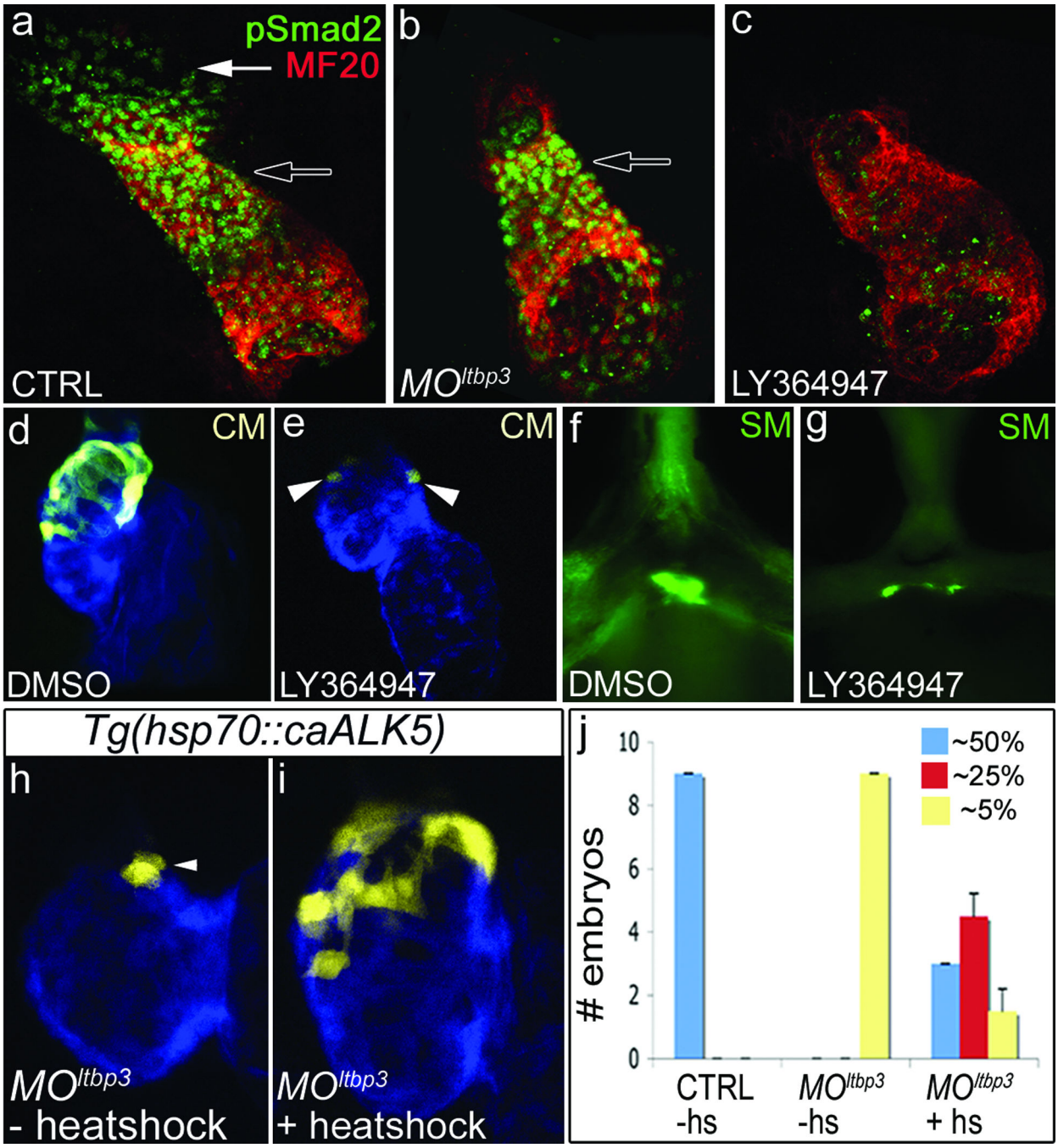

Figure 4. Diminished TGFβ signaling underlies the *MO*^{ltbp3} cardiovascular phenotypes

a–c, Heart tube regions in 24 hpf control, *MO*^{ltbp3}, and LY364947-treated embryos co-stained with a pSmad2 antibody and a muscle-specific antibody (MF20) that recognizes cardiomyocytes (n =20/20 for **a**, n=11/11 for **b**, n=15/15 for **c**). Black and white arrows highlight the heart tube and extra-cardiac pSmad2^{+} cells respectively. **d, e,** 72 hpf hearts in *Tg*(*ltbp3::TagRFP2Acre); Tg(cmlc2::CSY)* embryos treated with DMSO or LY364947 (n=8/8 per group); CM=cardiomyocytes. **f, g,** OFT region in 60 hpf embryos treated with DMSO or LY364947 and immunostained for Eln2 epitopes (n=20/20). SM=smooth muscle

precursors. **h–j,** Control and *MO^{ltbp3} Tg(ltbp3::TagRFP2Acre); Tg(cmlc2::CSY); Tg(hsp70::caALK5)* embryos were heat shocked (+hs) or not (−hs) and evaluated visually at 72hpf. Graph in (**k**) indicates the number of embryos in each experimental group that expressed ZsYellow protein in the distal ~50% (full rescue), ~25% (partial rescue), or ~5% (no rescue) of the ventricle. Shown in (**j**) is a heart that is partially rescued.